

Contrast Enhancement in Poor Visibility Conditions Using Guided Filtering

Danish Ali CHOWDHRY, Adil Masood SIDDIQUI, Imran TOUQIR

Dept. of Electrical Engineering, Military College of Signals,
National University of Sciences and Technology (NUST), Pakistan

{dac_msee17, dradil, imrantqr}@mcs.edu.pk

Abstract. *In this paper, extraction of atmospheric veil is proposed to enhance the contrast of the images captured under poor visibility conditions. The method based on guided filtering can accurately recover hidden edges, maintain structural similarity to input image and it is effective for both color and gray level images. The proposed algorithm works without prior information about the scene and its complexity is linear function of the input image size. Experimental comparisons with state of the art algorithms demonstrate that our approach can significantly enhance the contrast and restore the visibility in fine details.*

Keywords

Poor visibility conditions, atmospheric aerosols, contrast enhancement, atmospheric veil, guided filter, haze and fog removal.

1. Introduction

Most of the computer vision applications in outdoor environments such as automatic surveillance systems, object detection and tracking, object recognition, etc., are designed for clear weather. Bad weather conditions envisage difficulty in image analysis, processing and information extraction. Poor visibility that arises in bad weather is mostly due to presence of atmospheric aerosols such as haze, fog, mist, etc. These particles partially absorb and scatter the light reflected from the scene, resulting in image contrast degradation. Therefore contrast enhancement of such degraded outdoor images is highly desired.

Image contrast enhancement can be achieved by using either model or non-model based methods. Non-model based methods do contrast enhancement without knowing the cause of image degradation whereas model based methods perform image restoration by reversing the underlying cause. Compared with non-model based, model based methods usually give natural results and retain the information contents of the image.

In the literature, various solutions have been proposed to improve the scene visibility. Shwartz [1] and Schechner [2]

enhance the visibility by using multiple images with different degrees of polarization. Polarization-based methods cannot be used on existing image databases because of the need of multiple image acquisition and dedicated hardware for rotating the polarizer filter [3]. Nayar and Narasimhan [4], [5] restored the contrast by using multiple input images of the same scene which were obtained under different weather conditions. This technique is effective but impractical because the images under different weather conditions are usually not available at the same time. Depth-based methods by Hautiere [6], Narasimhan [7] and Kopf [8] seek additional depth information either from user interactions or known three-dimensional models. These techniques resolve the problem of multiple images requirement, but availability of either three-dimensional models of the real world or expert interaction makes these schemes unsuitable for real-time applications.

Rao [9] proposed approaches based on physical model to restore the images and estimate the scatter coefficient. Although these schemes get good restoration result, they are iterative and require a minimum of 3 to 4 steps to converge. Zuo [10] introduced a non-iterative technique to blind restoration based on improved Self-deconvolving Data Reconstruction Algorithm (SeDDaRA) method. This method first extracts a point spread function directly from the degraded data in the frequency domain and then uses Wiener filter to restore it.

Recently, single image contrast enhancement approaches by Fattal [11], He [12] and Tan [13] have been presented. These methods recover the contrast of weather-degraded input images using appropriate prior information or assumptions. All these current approaches fail when the image mismatches their prior or assumption. The main disadvantage of these algorithms is their time consumption. Average time taken for a 600 x 400 image is around 30-40 seconds, 10-20 seconds and 5-7 minutes in [11], [12], [13] respectively. Tarel [14] proposed a fast algorithm for visibility restoration from a single image. This algorithm is based on median filtering and it restores the visibility by inferring the atmospheric veil. Its computation time is less than a second for a 598 x 396 image on 3 GHz dual core processor [15] and claims to have similar or in some cases better results when compared to [11], [12], [13]. However,

this algorithm does not improve the visibility in small details of the image.

In this paper, we proposed a new method of inferring the atmospheric veil. The proposed algorithm is also fast since the time required is linear in amount of pixels. Moreover, the algorithm works without prior information or assumption and is applicable for both color and gray level images. Results show the ability of the method to successfully enhance the contrast of weather-degraded images in fine details.

The rest of the paper is organized as follows: Section 2 briefly describes preliminaries consisting of optical imaging model, atmospheric veil inference and guided image filtering. In Section 3, framework of our approach and steps of proposed method are elaborated. Section 4 verifies the validity of the proposed algorithm through experimental comparisons, followed by the conclusion in Section 5.

2. Preliminaries

2.1 Optical Imaging Model

Poor visibility is mostly due to presence of atmospheric aerosols which partially absorb and scatter the reflected light from the scene before reaching the camera. In computer vision and computer graphics, the optical imaging model is widely used to approximate the formation of image taken in poor visibility conditions. It can be mathematically described for RGB and gray level images by [11], [12], [13], [14]:

$$I^c(x) = J^c(x)t(x) + A(1-t(x)) \quad (1)$$

where x indicates the location of a pixel, I is the observed image, A is the global atmospheric light, J stands for the scene radiance, t is the medium transmission and superscript c represents one of the RGB color channel.

In (1), the first term $J(x)t(x)$ represents the directly attenuated component and the second term $A(1-t(x))$ is called the airlight. Pictorial description of the model is shown in Fig. 1. Assuming homogenous atmosphere constraint, we have the transmission expressed as:

$$t(x) = e^{-\beta d(x)} \quad (2)$$

where superscript β is the atmospheric attenuation coefficient and d is the scene depth. Putting $t(x)$ in (1):

$$I^c(x) = J^c(x)e^{-\beta d(x)} + A(1-e^{-\beta d(x)}). \quad (3)$$

This indicates that the scene radiance is attenuated, exponentially with the scene depth d . Thus, in order to recover the scene radiance using optical model, atmospheric light and depth / transmission map are frequently used.

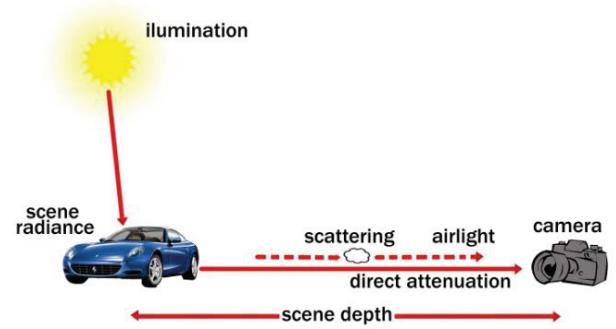


Fig. 1. The pictorial description of the optical imaging model.

2.2 Atmospheric Veil Inference

Visibility restoration is an ill-posed task as it is dependent on the unknown depth information. In order to achieve it, optical imaging model can be reframed as:

$$I^c(x) = J^c(x) \left(1 - \frac{A(1-e^{-\beta d(x)})}{A} \right) + A(1-e^{-\beta d(x)}). \quad (4)$$

Let the atmospheric veil intensity V be described as [14]:

$$V(x) = A(1-e^{-\beta d(x)}). \quad (5)$$

Putting (5) into (4), we can model the observed image in terms of atmospheric veil as:

$$I^c(x) = J^c(x) \left(1 - \frac{V(x)}{A} \right) + V(x). \quad (6)$$

Here we equivalently seek to infer the atmospheric light and atmospheric veil out of the observed image to get the restored image.

2.3 Guided Image Filtering

The guided filter [16] is an explicit image filter; it generates the filtering output by considering the contents of a guidance image that can be the input image itself or another different image. The filter has the edge-preserving smoothing property and its computational complexity is independent of the filtering kernel size.

The output of the guided filter z is a linear transformation of guidance image G in a square window ω_n of radius r centered at the pixel n . The linear coefficients p_n and q_n are determined in a way that minimizes the difference between z and the input image h , solution to which is:

$$p_n = \frac{1}{|\omega|} \frac{\sum_{m \in \omega_n} G_m h_m - \mu_n \bar{h}_n}{\sigma_n^2 + \epsilon}, \quad (7)$$

$$q_n = \bar{h}_n - p_n \mu_n. \quad (8)$$

The coefficients are assumed to be constant in ω_n . Here, σ_n^2 and μ_n are the variance and mean of G in ω_n , ε is the regularization parameter that prevents p_n from approaching infinity, $|\omega|$ is the cardinality of ω_n and

$$\bar{h}_n = \frac{1}{|\omega|} \sum_{m \in \omega_n} h_m$$

is the mean of h in ω_n . Finally, after finding linear coefficients from all the local windows in the entire image, filter output is computed by:

$$z_m = \frac{1}{|\omega|} \sum_{n: m \in \omega_n} (p_n G_m + q_n). \quad (9)$$

3. Proposed Methodology

3.1 Atmospheric Light Estimation

There are many techniques existing in the literature to estimate the atmospheric light A . The pixel with the highest intensity value is used as A by Tan [13], Fattal [11] computed A by solving an optimization problem, Tarel [14] directly set A to (1, 1, 1) after performing white balance in preprocessing stage and He [12] picks the highest intensity pixel equals to A among the top 0.1% brightest dark channel pixels. In our paper, we apply white balance by assuming that atmospheric light has larger intensity than that of any other pixel.

3.2 Atmospheric Veil Extraction

The physical properties of the atmospheric veil are subject to two constraints [14]. For an observed image $I(x)$ it is non-negative and being pure white, it cannot be higher than the minimum of the components of $I(x)$. Mathematically, these constraints can be expressed by a single inequality as $0 \leq V(x) \leq D(x)$. We thus computed image of the whiteness $D(x)$ within the observed image defined as the image of the minimal component of $I(x)$. For each pixel, it is defined as:

$$\text{For RGB image: } D(x) = \min(I(x)), \quad (10)$$

$$\text{For gray level image: } D(x) = I(x). \quad (11)$$

When the airlight is pure white the atmospheric veil adds whiteness to the image, the amount of whiteness added depends on the depth of the object. Because the whiteness gives information about the depth and the depth is proportional to the atmospheric veil, it is possible to base the atmospheric veil on image of the whiteness. Therefore, atmospheric veil is extracted in a robust way from $D(x)$ by following the steps shown in Fig. 2.

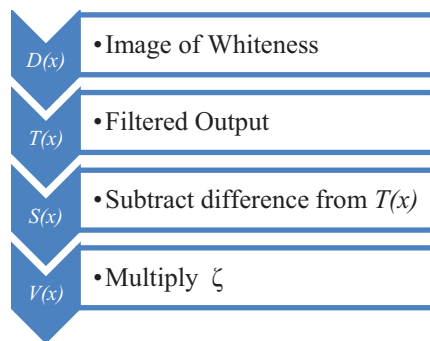


Fig. 2. Steps of atmospheric veil extraction.

Firstly, guided filter [16] is employed on $D(x)$ to obtain the filtered image of whiteness $T(x)$. We used guided filtering because it performs smoothing by preserving large jumps along edges which is necessary for the image restoration. In contrasted texture image portions, the absolute difference between $D(x)$ and $T(x)$ yield low values. This difference is subtracted from $T(x)$ so that $T(x)$ in these areas is not affected too much. Guided filter is applied on the absolute difference for making the scheme robust to outliers. Finally, $V(x)$ is inferred by multiplying a constant parameter ξ after obtaining the smallest entries from $S(x)$ or $D(x)$. The values of $S(x)$ do not necessarily respect the constraints on the veil and thus are thresholded. Mathematically the atmospheric veil is estimated by:

$$V(x) = \xi (\max(\min(S(x), D(x)), 0))$$

where

$$S(x) = T(x) - \text{guided}(|D - T|)(x)$$

and

$$T(x) = \text{guided}(D)(x) \quad (12)$$

where ξ determines the percentage of restoration ($0 \leq \xi \leq 1$). Atmospheric veil using median filter [14] is unable to recover the visibility of aerosol degraded images in fine details. Hence, in this work, the method of extracting the atmospheric veil is modified. It is achieved using guided filter which avoids the gradient reversal artifacts that may appear in detail enhancement. Guided filter is fast and non-approximate linear-time algorithm [16] and it improves the accuracy of atmospheric veil in a better way. Fig. 3 shows a hazy image, filtered version $T(x)$ and its corresponding estimated atmospheric veil.

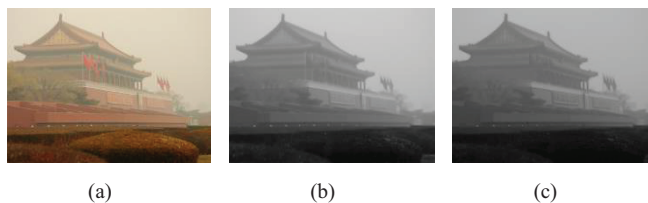


Fig. 3. (a) Input hazy image. (b) Filtered image of whiteness. (c) Estimated atmospheric veil.

3.3 Recovering the Scene Radiance

Given the atmospheric light and atmospheric veil, we can recover the scene radiance from (6) as:

$$J^c(x) = \frac{I^c(x) - V(x)}{1 - \frac{V(x)}{A}} \quad (13)$$

4. Experimental Comparisons

Several experimental comparisons are conducted for proposed contrast enhancement algorithm, which is controlled by following three parameters: ε which is the regularization parameter, r is the radius of local window for guided filter and ξ is to control the strength of restoration.

4.1 Qualitative Comparisons

Fig. 4 warrants the use of guided filter in this paper. Tarel [14] uses geometric criterion to decide whether the observed white region is due to the fog or the object’s color. As a result it can be seen that fog is not removed between the small leaves. Using the same criterion with guided filter in Fig. 4(c), we successfully recover fine details by removing the fog between the small portions of highlighted rectangles and circles in Fig. 4(b) and 4(c).

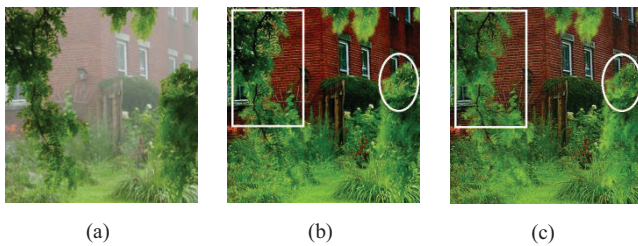


Fig. 4. (a) Input foggy image. (b) Restored image using median filtering [14]. (c) Restored image using guided filtering

Fig. 5 allows the comparison of our result with five most popular algorithms of visibility enhancement under bad weather conditions [8], [11], [12], [13], [14]. Kopf [8] utilizes 3D models of the scene, this information may come from Google Earth and satellite images. Fattal’s [11] work is based on color information and the algorithms of He [12], Tan [13] and Tarel [14] are based on geometric criterion. It is obvious from the results that our algorithm significantly overcomes the dense fog on the mountains,

whereas there is still a small amount of haze left to be removed using all other algorithms. Additionally, colors produced by He [12] and Tan [13] are somewhat artificial, whereas our result looks more realistic and the colors remained consistent with the input foggy image.

The comparison of our method with improved SeDDaRA method [10] on real turbulent degraded image has been shown in Fig. 6. We adopted the same pre-

processing used in [10] prior to our algorithm. It is evident from the results that the proposed scheme produces comparable results.

4.2 Quantitative Comparisons

We adopted the approach of Hautiere [17] to quantitatively evaluate the quality of enhancement. Here, we transform the color to gray level images and then compare gray level images by determining the three visual descriptors: e (rate of new visible edges), η (percentage of pixels which becomes completely black or completely white after enhancement) and Ω (mean ratio of the gradients at visible edges). We calculated these descriptors for five approaches presented by Kopf [8], Fattal [11], Tan [13], He [12] and Tarel [14] on five images ny12, ny17, y01, y16 and stad1.

Tab. 1 contains the numerical values of rate of new visible edges e after restoration, which demonstrates that there is a huge improvement to the rate of restored edges when compared with five known state of the art visibility restoration algorithms. Tab. 2 shows the percentage of pixels η which become completely black or completely white after the contrast restoration. Compared to the others, our algorithm makes no pixel either completely black or completely white after the restoration. Tab. 3 gives the mean ratio Ω of the gradients at visible edges which estimate the average visibility enhancement. One can notice that, most of our results are either similar or better than Kopf, Fattal and He but less enhanced than Tan and Tarel. However, Tan’s method faces problem of producing oversaturated colors in the results and Tarel’s work is not able to remove the haze in fine details.

e	Kopf	Fattal	Tan	He	Tarel	Our
ny12	0.0361	-0.0538	-0.0835	0.0482	0.1450	0.408
ny17	0.0169	-0.1060	-0.0412	0.0232	0.1104	0.405
y01	0.0947	0.0864	0.1219	0.1426	0.2092	0.435
y16	0.0009	0.0582	-0.0165	0.1314	0.2406	0.637
stad1	-	0.237	0.295	0.368	0.397	0.531

Tab. 1. Rate of new visible edges.

η	Kopf	Fattal	Tan	He	Tarel	Our
ny12	0.17587	0.6409	1.836	0.0002	0.0	0.0
ny17	0.12347	1.6988	0.7653	0.0136	0.00013	0.0
y01	0.01944	0.1128	0.3875	0.0136	0.0	0.0
y16	0.28347	0.1491	0.4474	0.1522	0.00045	0.0
stad1	-	0.3945	1.9566	0.0083	0.0	0.0

Tab. 2. Percentage of pixels which becomes completely black or completely white after contrast enhancement.

Ω	Kopf	Fattal	Tan	He	Tarel	Our
ny12	1.4091	1.2875	2.1802	1.3979	1.7628	1.619
ny17	1.6136	1.5346	2.19	1.6297	1.7057	1.568
y01	1.6362	1.2152	2.2283	1.3134	1.9903	1.62
y16	1.3456	1.2033	2.0602	1.3674	1.9583	1.671
stad1	-	1.867	4.359	2.191	1.408	1.56

Tab. 3. Mean ratio of the gradients at visible edges.

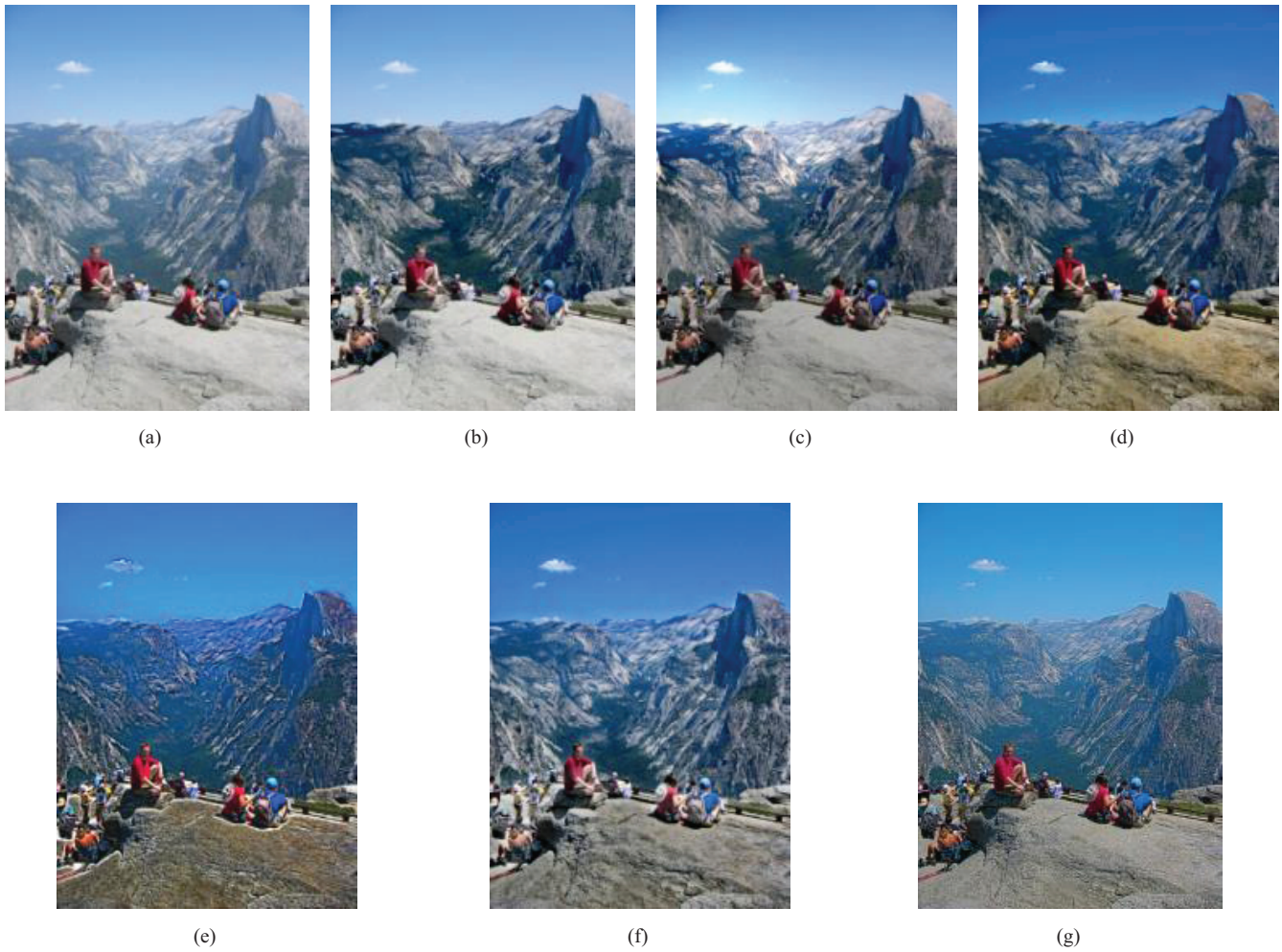


Fig. 5. Comparison with conventional methods. (a) Observed image. (b) - (f) Results obtained by Kopf [8], Fattal [11], He [12], Tan [13], Tarel [14]. (g) Our result with $\varepsilon = 0.01$, $r = 2$ and $\xi = 0.9$.

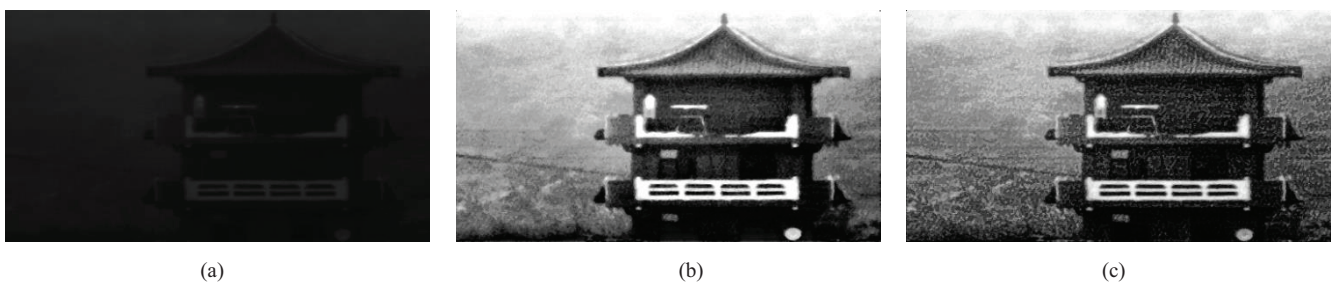


Fig. 6. Turbulence degraded image restoration. (a). Real turbulence degraded image; (b). Restored result by Zuo [10]; (c). Our result with $\varepsilon = 0.01$, $r = 2$ and $\xi = 0.9$.

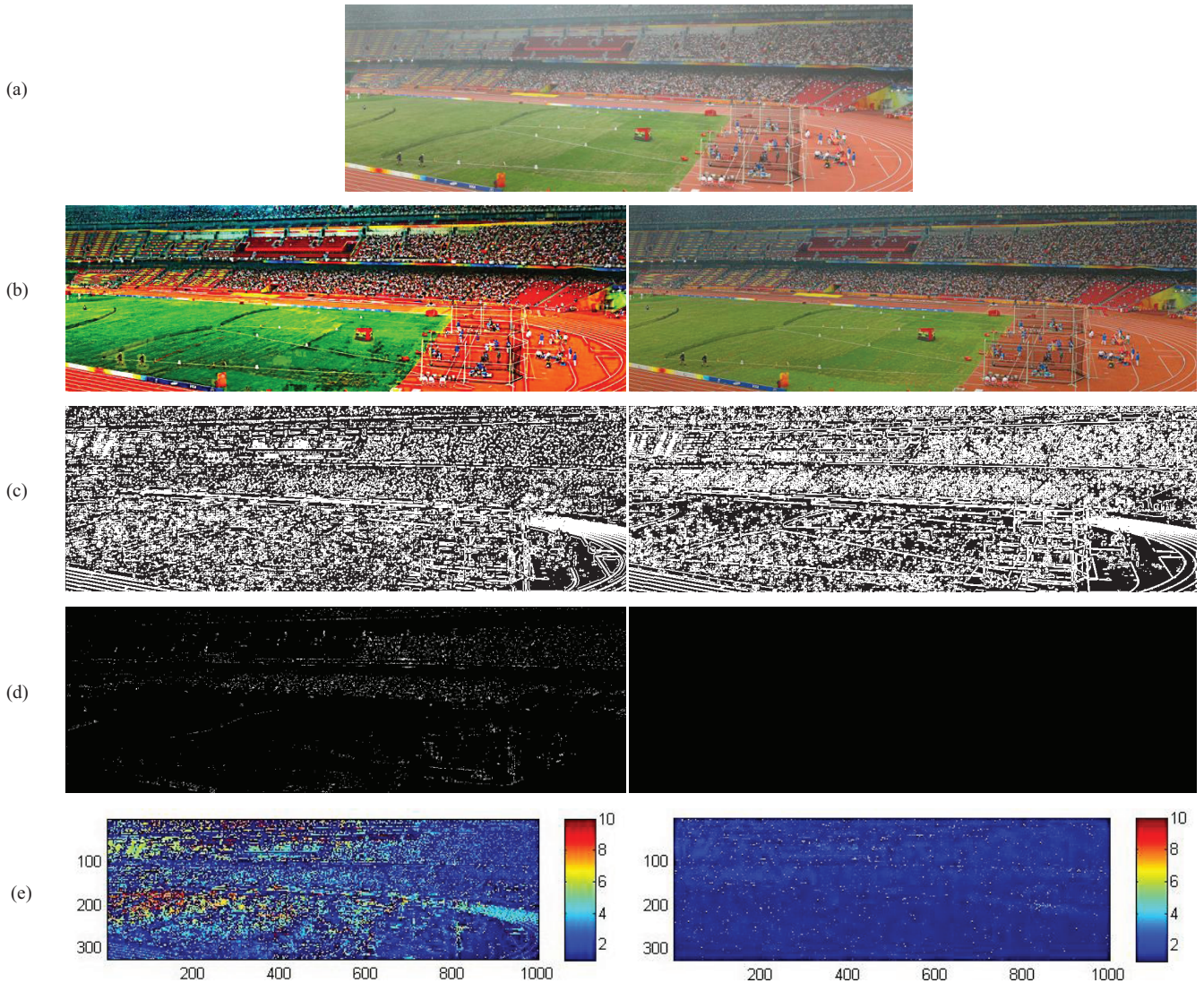


Fig. 7. Comparison with Tan's work [13]. (a) Input image. (b) Restored images. (c) Map of visible edges in the restored image. (d) Map of pixels becoming completely black or completely white. (e) Map of ratio of the gradients at visible edges. Left and right columns show Tan and our results respectively.

Fig. 7 shows the comparison of our approach with Tan's work [13] on stad1 image. Maps of visible edges of the restored images in Fig. 7(c) indicate that our method recovers more detail by restoring 169726 edges where Tan's method restores only 143501 edges. The perturbed pixels in Fig. 7(d) demonstrate that our result make no pixel either completely black or completely white. In Fig. 7(e), is shown the maps of ratio Ω of the gradients at visible edges for Tan and our algorithm which indicates that contrast has been amplified too strongly by Tan, which results in oversaturated colors of the restored image.

Apart from improving visibility of images captured in poor visibility conditions, a contrast enhancement method must also have to provide good structural similarity (SSIM) with the contrast-degraded images. Thus we also use the method proposed by Wang [18] to measure the SSIM between the degraded images and the restored results by Tan [13], Tarel [14] and ours. Fig. 8 shows that SSIM indexes for our results are more than that of Tan and

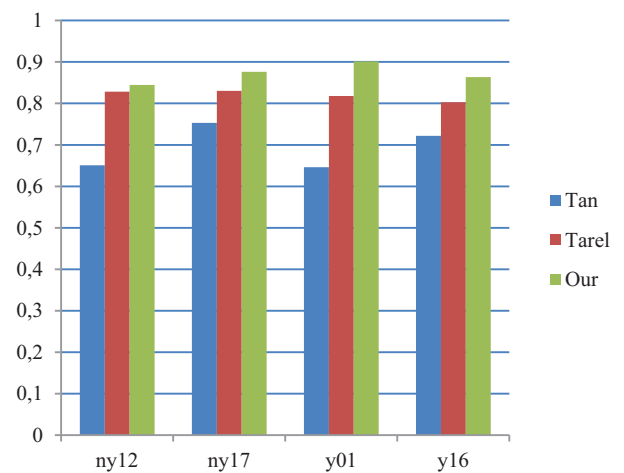


Fig. 8. SSIM index for Tan, Tarel and our results on four images.

Tarel's results. This illuminates that our method bring less halos and artifacts when compared to two methods [13], [14].

Qualitative and quantitative comparisons not only support each other but also verify that our results can produce huge rate of new visible edges and good SSIM by avoiding oversaturation in colors.

5. Conclusion

An algorithm that improves the contrast of aerosol degraded color and gray scale images, is presented. Our proposed method, based on guided filter, can unveil the details even in heavily hazy region without leaving any prominent halos along edges. Additionally, the algorithm does not need any human intervention and its complexity is a linear function of the number of input image pixels.

Acknowledgements

The authors gratefully thank the anonymous reviewers for their valuable comments that led to improvement of the paper quality.

References

- [1] SHWARTZ, S., NAMER, E., SCHECHNER, Y. Y. Blind haze separation. In *Proceedings of IEEE Conference on Computer Vision and Pattern Recognition (CVPR)*. New York (USA), 2006, vol. 2, p. 1984 -1991.
- [2] SCHECHNER, Y. Y., NARASIMHAN, S. G., NAYAR, S. K. Instant dehazing of images using polarization. In *Proceedings of IEEE Conference on Computer Vision and Pattern Recognition (CVPR)*. Kauai (USA), 2001, vol. 1, p. 325 - 332.
- [3] YOON, I., KIM, S., KIM, D., HAYES, M. H., PAIK, J. Adaptive defogging with color correction in the HSV color space for consumer surveillance system. *IEEE Transactions on Consumer Electronics*, 2012, vol. 58, no. 1, p. 111 - 116.
- [4] NAYAR, S. K., NARASIMHAN, S. G. Vision in bad weather. In *Proceedings of Seventh International Conference on Computer Vision (ICCV)*. Corfu (Greece), 1999, vol. 2, p. 820 - 827.
- [5] NARASIMHAN, S. G., NAYAR, S. K. Contrast restoration of weather degraded images. *IEEE Transactions on Pattern Analysis and Machine Intelligence (TPAMI)*, 2003, vol. 25, no. 6, p. 713 - 724.
- [6] HAUTIERE, N., TAREL, J., AUBERT, D. Toward fog-free invehicle vision systems through contrast restoration. In *IEEE Conference on Computer Vision and Pattern Recognition (CVPR)*. Minneapolis (USA), 2007, p. 1 - 8.
- [7] NARASIMHAN S. G., NAYAR, S. K. Interactive deweathering of an image using physical models. *Proceedings of IEEE ICCV Workshop on Color and Photometric Methods in Computer Vision (CPMCV)*. 2003.
- [8] KOPF, J., NEUBERT, B., CHEN, B., COHEN, M., COHEN-OR, D., DEUSSEN, O., UYTTENDAELE, M., LISCHINSKI, D. Deep photo: Model-based photograph enhancement and viewing. *ACM Transactions on Graphics (SIGGRAPH Asia'08)*, 2008, vol. 27, no. 5, p. 116:1 - 116:10.
- [9] RAO, R., SEUNGSIN, L. Algorithms for scene restoration and visibility estimation from aerosol scatter impaired images. In *IEEE International Conference on Image Processing (ICIP)*. Genoa (Italy), 2005, vol. 1, p. 1-929 - 1-932.
- [10] ZUO, H., ZHANG, Q.,RUJIN Z. An efficiency restoration method for turbulence-degraded image base on improved SeDDaRa method. *International symposium on Photoelectronic detection and Imaging*. Beijing (China), 2009.
- [11] FATTAL, R. Single image dehazing. *ACM Transactions on Graphics (SIGGRAPH'08)*, 2008, vol. 27, p. 1 - 9.
- [12] HE, K., SUN, J., TANG, X. Single image haze removal using dark channel prior. *IEEE Transactions on Pattern Analysis and Machine Intelligence (TPAMI)*, 2011, vol. 33, no. 12, p. 2341 - 2353.
- [13] TAN, R. T. Visibility in bad weather from a single image. In *Proceedings of IEEE Conference on Computer Vision and Pattern Recognition (CVPR)*. Anchorage (USA), 2008, p. 1 - 8.
- [14] TAREL, J.-P., HAUTIERE, N. Fast visibility restoration from a single color or gray level image. In *International Conference on Computer Vision (ICCV)*. Kyoto (Japan), 2009.
- [15] PARIJS, Y. *Video Based Fog Removal*. Thesis Number: ICA-3369234. Utrecht (The Netherlands): University of Utrecht, 2012.
- [16] HE, K., SUN, J., TANG, X. Guided image filtering. *IEEE Transactions on Pattern Analysis and Machine Intelligence (TPAMI)*, 2013, vol. 35, no. 6, p. 1397 - 1409.
- [17] HAUTIERE, N., TAREL, J.-P., AUBERT, D., DUMONT, E. Blind contrast enhancement assessment by gradient ratioing at visible edges. *Image Analysis & Stereology Journal*, 2008, vol. 27, no. 2, p. 87 - 95.
- [18] WANG, Z., BOVIK, A. C., SHEIKH, H. R. Image quality assessment: from error visibility to structural similarity. *IEEE Transactions on Image Processing*, 2004, vol. 13, no. 4, p. 600 - 612.